Vibrationally Resolved Photoelectron Spectroscopy of MgO^- and ZnO^- and the Low-Lying Electronic States of MgO, MgO^-, and ZnO

Jeong Hyun Kim,[†] Xi Li, and Lai-Sheng Wang*

Department of Physics, Washington State University, 2710 University Drive, Richland, Washington 99352 and W. R. Wiley Environmental Molecular Sciences Laboratory, Pacific Northwest National Laboratory, MS K8-88, P.O. Box 999, Richland, Washington 99352

Helen L. de Clercq,[‡] Charles A. Fancher,[§] Owen C. Thomas, and Kit H. Bowen*

Department of Chemistry, The Johns Hopkins University, Baltimore, Maryland 21218

Received: January 25, 2001; In Final Form: May 8, 2001

Vibrationally resolved photoelectron spectra of MgO^- and ZnO^- have been recorded at several photon energies under varied experimental conditions. Peaks in these highly structured spectra have been assigned to photodetachment transitions from the MgO^- and ZnO^- ground state ($X^2\Sigma^+$) to vibrational progressions in the ground and several low lying neutral excited states. In addition, a high-temperature MgO^- spectrum shows spectral features due to photodetachment from an excited electronic state of the MgO^- anion, which has been assigned to an $A^2\Pi$ anionic state. From the MgO^- spectra, the electron affinity of the MgO ground state ($X^1\Sigma^+$) is determined to be 1.630 (0.025) eV. Four electronic excited states of MgO, $a^3\Pi$, $A^1\Pi$, $b^3\Sigma^+$, and $B^1\Sigma^+$, were found to lie 2510, 3390, 8390, and 20 000 cm^{-1} above the $X^1\Sigma^+$ neutral ground state, respectively. The excited MgO^- $A^2\Pi$ anion state was found to lie 4791 cm^{-1} above the MgO^- $X^2\Sigma^+$ anion ground state. The photoelectron spectra of ZnO^-, presented here at higher photon energies, extend a previous photoelectron study by Fancher et al. to the first two excited neutral states, $a^3\Pi$ and $A^1\Pi$, which have been found to lie 2460 and 4960 cm^{-1} above the $X^1\Sigma^+$ ground state, respectively. From Franck−Condon analyses of the well-resolved vibrational progressions for each electronic transition, equilibrium internuclear distances and fundamental vibrational frequencies of the MgO and ZnO neutral electronic states were determined. Moreover, because the sources employed produced vibrationally hot anions, the bond length and vibrational frequencies of both the MgO^- ground and excited states were found from the vibrational hot band transitions.

1. Introduction

MgO and ZnO are two relatively simple diatomic molecules and they have been found to have $X^1\Sigma^+$ ground states.[1,2] However, there have been vigorous debates on the nature of the ground state due to the presence of a number of low-lying electronically excited states.[1,3−6] In particular, MgO is distinguished from other alkaline earth metal oxides in that it has closely lying Π excited states.[4,7] Up to the early 1970s the experimentally known electronic transitions for MgO were those involving the three lowest singlet states, $X^1\Sigma^+$, $A^1\Pi$, and $B^1\Sigma^+$.[10] Because the $A^1\Pi$ state was found to lie only ∼3500 cm^{-1} above the $X^1\Sigma^+$ state, it was proposed that the triplet counterpart to the $A^1\Pi$ state, the $a^3\Pi$ state, might lie below the $X^1\Sigma^+$ state. In 1972, Schamps and Lefebvre-Brion performed LCAO-MO SCF calculations on the electronic states of MgO and predicted that a proper consideration of correlations in the electronic configurations indicated a $X^1\Sigma^+$ ground state.[3] In the experiments that followed these studies, the $a^3\Pi$ state was investigated through weak spin-forbidden optical transitions whose oscillator strengths are borrowed from allowed transitions between singlet states.[1,9,10] In 1977, Ikeda, Wong, Harris, and Field investigated the $a^3\Pi$−$X^1\Sigma^+$ perturbations in photoluminescence spectra of MgO and provided an estimated set of spectroscopic constants for the $a^3\Pi$ state.[1] Their results also provided experimental proof for the $X^1\Sigma^+$ ground state. More recently, Field and co-workers performed rotational analysis of the $B^1\Sigma^+$−$a^3\Pi$ (0,0) and (0,1) intercombination bands measured by fluorescence excitation spectroscopy.[11] This was followed by Faraday laser magnetic resonance spectroscopy experiments of Mürtz et al., who reported the first direct observation of transitions between the $X^1\Sigma^+$, $a^3\Pi$, $B^1\Sigma^+$, and $A^1\Pi$ states.[9,10] These studies also found an $X^1\Sigma^+$ ground state and furnished rotational constants and perturbation parameters for the $X^1\Sigma^+$, $a^3\Pi$, and $B^1\Sigma^+$ states. Of the low-lying states of MgO, this left only the triplet counterpart to the $B^1\Sigma^+$ state, i.e., the $b^3\Sigma^+$ state, to be investigated. Its spectroscopic properties were given by several theoretical predictions. Bauschlicher, Lengsfield, Silver, and Yarkony performed MCSCF/CI calculations for the low-lying states of MgO and estimated the transition energy (T_e) of the $b^3\Sigma^+$ state to be 8300 ± 800 cm^{-1}.[6] A similar value, 8414 cm^{-1}, was found by Thümmel et al., who calculated the potential energy curves for the low-lying electronic states of MgO using a multireference configuration interaction (MRD CI) method.[12] Experimentally, Ip et al. analyzed intercombination systems related to the $a^3\Pi$ state and showed a significant effect from

* Corresponding authors.
[†] Visiting from School of Chemistry, Seoul National University, Seoul 151-742, Korea.
[‡] Present address: Department of Chemistry, Howard University, Washington, DC 20059.
[§] Present address: Stanford Research Systems, Sunnyvale, CA 94089.

10.1021/jp010331d CCC: $20.00
Published on Web 05/23/2001

interactions with the $X^1\Sigma^+$ and $B^1\Sigma^+$ states on the Λ-doubling in the $a^3\Pi$ state, confirming indirectly the location of the $b^3\Sigma^+$ state.[11]

In addition to spectroscopic interest, the importance of magnesium oxide as a catalyst in hydrocarbon reactions has motivated a number of thermochemical investigations upon the bulk solid, the bulk surfaces, particles, and more recently, clusters. To understand these processes at a molecular level, and to help model them theoretically, an understanding of the monomer is necessary. Consequently, several thermochemical studies have been conducted on molecular magnesium oxide to determine its dissociation energy, D_0. Most reported experimental values from recent decades are greater than 3.5 eV. There have been, however, controversies regarding the purity of the samples used for the techniques employed, such as flame photometry and Knudsen cell mass spectrometry.[13] Ab initio calculations by Langhoff et al. found $D_0 = 2.71$ eV, measured relative to the lowest energy dissociation asymptote, Mg ($3s^2$, ^1S) + O ($2p,^4$ ^3P), a result smaller than the previously reported values.[14] In a Fourier transform mass spectrometry examination of MgO and MgOH by Operti et al., the D_0 of MgO^+ cation and the ionization potential of MgO neutral were measured by photodissociation and charge-transfer reactions, respectively.[15] These measurements were used with published enthalpies of formation to find $D_0 = 2.56$ eV through a thermochemical cycle. Note, however, that while these investigations have in general found the dissociation energy relative to the ground state separated atoms, the $X^1\Sigma^+$ molecular ground state arises from ionic and covalent separated atom asymptotes, Mg^+ ($3s^1$, ^2S) + O^- ($2p,^5$ ^2P) and Mg ($3s^2$, ^1S) + O ($2p,^4$ ^1D). Both asymptotes lie at energies higher than the ground state Mg ($3s^2$, ^1S) + O ($2p,^4$ ^3P) separated atoms. Rather, the ground state separated atoms are associated with the excited molecular state, $a^3\Pi$. Accordingly, the electronic structure of MgO has been considered a matter of significance in thermochemical, as well as spectroscopic, aspects.

The behavior of the group II-B metals ($d^{10}s^2$) is similar in many respects to that of the alkaline earth metals. However, due to the difficulty in thermally generating gas-phase ZnO, (solid ZnO sublimes by dissociation to its elements[16]), there are only a few experimental studies of the ZnO molecule. Thermochemical properties of the ZnO molecule have been investigated by measurements of the reaction of Zn with various oxidants. The kinetic energy dependence of the chemiluminescence from the oxidation reaction of Zn atoms with N_2O was studied by Wicke, who estimated the lower limit of the dissociation energy of ZnO to be 2.8 eV from a threshold in the chemiluminescent reaction cross section.[17] However, an earlier high-temperature mass spectrometry investigation set the upper limit to the dissociation energy at 2.86 eV, and theoretical studies at the time also found the dissociation energy to be well below 2.8 eV. In 1986, Bauschlicher and co-workers investigated the low-lying electronic states of ZnO, $X^1\Sigma^+$, $a^3\Pi$, $A^1\Pi$, and $b^3\Sigma^+$, using CI and coupled pair formalism (CPF) methods and predicted the dissociation energy for the $X^1\Sigma^+$ state, $D_e = 1.20$ eV (relative to ground state atoms).[2] Subsequent thermochemical experiments using a guided ion-beam mass spectrometry technique on the reaction of Zn^+ and NO_2 by Armentrout and co-workers yielded a dissociation energy of 1.61 eV for neutral ZnO.[18] The apparent discrepancy from Wicke's lower limit was explained by noting that an electron in the fully occupied 4s and 3d orbitals of the ground state zinc atom should be excited to a 4p orbital for bonding, which implied a smaller dissociation energy for ZnO compared with the other transition metal oxides, such as the well-established value (~2.8 eV) for CuO.[13]

Until recently, spectroscopic measurements of ZnO were limited to the 1980 study of the ZnO molecule in a solid nitrogen matrix by Prochaska and Andrews,[19] and were later revised by Chertihin and Andrews in a solid argon matrix study in 1997.[20] The first spectroscopic measurements of the isolated gas-phase molecule were reported in 1997 by Fancher, de Clercq, Thomas, Robinson, and Bowen, who measured the photoelectron spectrum of ZnO^- at 2.707 eV photon energy (457.9 nm).[21] Fancher et al. observed a single vibrational progression for the neutral ground state ($X^1\Sigma^+$) and obtained the electron affinity of ZnO (2.088 ± 0.010 eV). A Franck−Condon analysis yielded the fundamental vibrational frequency for both the neutral and anion ground state and the bond length and well depth for the anion. In an accompanying paper by Bauschlicher and Partidge, ab initio calculations on the electronic structure of ZnO and ZnO^- were performed at the coupled cluster level with single and double excitations and noniterative inclusion of all triple excitations (CCSD(T)).[22] The calculated ZnO and ZnO^- spectroscopic constants and electron affinity were found to be in good agreement with the accompanying experimental measurements, while the well depth of the neutral ($D_0 = 1.63$ eV) reproduced the earlier experimental value of 1.61 eV, determined experimentally by Armentrout and co-workers.

In the work reported here, the ZnO^- photoelectron spectra are measured at 532 and 355 nm and extend the earlier photoelectron study of ZnO^- to the $a^3\Pi$ and $A^1\Pi$ excited states of ZnO. The current report represents the first experimental measurements of these states for the ZnO molecule. The photoelectron spectrum of MgO^- at 532 nm was reported in our recent study of a series of $(MgO)_n$ ($n = 1-5$) clusters.[23] The MgO^- photoelectron spectra presented in this paper combine two separate experimental investigations, covering a wide photon energy range and various experimental conditions. Four low-lying electronic states of MgO ($a^3\Pi$, $A^1\Pi$, $b^3\Sigma^+$, and $B^1\Sigma^+$) are observed and reported here for the first time, in addition to the observation of the first excited state of the MgO^- anion.

The MgO^- photoelectron spectra measured by The Johns Hopkins University (JHU), and the Pacific Northwest National Laboratory and Washington State University (PNNL/WSU) research groups have been collected under significantly different experimental conditions in both the photon energy range and anion production. Most noticeably, the two ion sources employed have produced MgO^- anions with dramatically different vibrational temperatures. The 488 nm spectrum measured at JHU includes photodetachment transitions from the ground-state anion to the $X^1\Sigma^+$, $a^3\Pi$, and $A^1\Pi$ neutral electronic states. In addition, the spectrum contains a significant amount of vibrational hot band transitions, which provide vibrational frequencies for the anion ground state. However, a large number of hot bands, interspersed with transitions from the ground state, makes Franck−Condon modeling difficult at the instrumental resolution of 0.023 eV. This problem was amplified in the case of MgO, where the neutral electronic states are close enough that their vibrational progressions overlap. A preliminary analysis assigned (0−0) peaks for the three neutral states, finding the electron affinity of the $X\ ^1\Sigma^+$ ground state and transition energies of the $a^3\Pi$ and $A^1\Pi$ states.[24] Ab initio calculations were performed by Bauschlicher and Partridge to assist in the interpretation of the JHU spectrum.[25] The results of these calculations were in good agreement with the experimental results for the (0−0)

photodetachment transitions to the MgO electronic states. Nevertheless, Franck−Condon modeling of the vibrational structure of the JHU spectrum was not successful at the time due to the extreme spectral congestion. Consequently, experimental values for the fundamental vibrational frequencies and bond lengths were not reported for these states and could not be compared to the calculated values. Interestingly, the JHU spectrum also contains features due to an excited electronic state of the anion, which, in the absence of a Franck−Condon analysis, were not assigned at that time.

The MgO^- photoelectron spectra measured at PNNL/WSU were taken at three photon energies, 2.331 (532 nm), 3.496 (355 nm), and 4.661 (266 nm) eV, and include photodetachment transitions from the ground-state anion to the $X^1\Sigma^+$, $a^3\Pi$, $A^1\Pi$, $b^3\Sigma$, and $B^1\Sigma$ neutral states. Detachment to the $b^3\Sigma$ state is the first direct measurement reported for this species. The ion source employed in these experiments produced a significantly smaller degree of vibrational excitation in the anion than that observed in the JHU spectrum. Consequently, the photodetachment transitions for all five neutral electronic states observed are well resolved. Even though the progressions for the first three low-lying neutral electronic states overlap to some degree, these spectra have been successfully modeled by Franck−Condon analyses, from which fundamental vibrational frequencies and equilibrium bond lengths have been obtained for the five neutral electronic states. From the moderate amount of hot-band transitions present, the spectroscopic constants of the anion were also obtained. The well-characterized spectroscopic constants for the neutral states derived from the PNNL/WSU spectra were then used to model the JHU spectrum to find spectroscopic constants for the excited state of the anion. Together the JHU and PNNL/WSU MgO^- photoelectron spectra reported here provide the electron affinity of the ground state, term values for the first four excited neutral states, and the first excited state of the anion. Franck−Condon analyses of the spectra provide fundamental vibrational frequencies and equilibrium bond lengths for all five neutral and both anion electronic states. The calculations performed by Bauschlicher and Partridge,[25] initially to assist in the interpretation of the JHU spectrum, are in good agreement with the combination of experiments performed at JHU and PNNL/WSU, and conclusions based on these calculations are consistent with those presented in this work.

2. Experimental Section

In this study, two representative methods in anion photoelectron spectroscopy were employed to investigate the electronic structure of MgO and ZnO. The experiments at PNNL/WSU were performed on an apparatus composed of a pulsed laser vaporization source, a time-of-flight (TOF) mass spectrometer, mass gate, momentum decelerator, and a magnetic-bottle TOF photoelectron spectrometer (MTOF−PES). At JHU, the photoelectron spectrum of MgO^- was obtained with a high-temperature continuous supersonic nozzle beam source, E × B Wein velocity mass filter, and a hemispherical electron energy analyzer. Here only brief descriptions will be presented. Details of each apparatus are given elsewhere.[24−28]

PNNL/WSU. To generate a sufficiently high-intensity beam of MgO^-, a carrier gas of 1% N_2O in He was used to react with laser-ablated Mg atoms in the laser vaporization cluster nozzle. The neutral and ion products formed via complex plasma reactions were co-expanded through a conical nozzle with the helium carrier gas and collimated by a skimmer. A 1 kV high-voltage pulse extracted anionic species from the beam perpendicularly into a TOF mass spectrometer. Using N_2O as the oxidant produced MgO^- diatomic with higher intensity than O_2 seeded gas, which produced mainly higher $Mg_nO_m^-$ clusters. ZnO^- anion was produced in a similar fashion, except that a 0.5% O_2 seeded He carrier gas was used. After anion production and mass selection, the monoxide anions of each metal were introduced into a photoelectron analyzer where they were illuminated with the output of a Nd:YAG laser. The photodetachment wavelengths were varied from 532 to 266 nm to adequately match the electronic states of interest. Typical resolution of this analyzer was ∼20 meV (fwhm) for 1 eV electron kinetic energy. The MTOF−PES collects emitted photoelectrons with high efficiency (∼100%). Electrons guided by a weak magnetic field were energy analyzed according to their flight time in a 3.5 m TOF tube. The photoelectron spectra of MgO^- and ZnO^- were calibrated to the known energy levels of Rh^- and Cu^-.[29,30] For the 532 and 355 nm experiments, the detachment laser and the vaporization laser were operated at 10 Hz. At 266 nm, the repetition rate of the detachment laser was doubled with the ion off at alternating laser pulses for background subtraction.

JHU. The beam line of the photoelectron spectrometer at JHU has been designed to accommodate a wide variety of ion sources. In these experiments, MgO^- anion was produced using a high-temperature supersonic nozzle ion source. This source has been constructed so that it may be operated continuously, producing a stable ion beam, over many hours, at temperatures reaching the softening point of stainless steel (∼900 °C). Magnesium metal (99.5% purity) was evaporated in the stainless steel oven at 850 °C under 200−300 Torr of preheated argon. The resultant Mg-seeded argon vapor was expanded supersonically through a 125 μm diameter nozzle, which is heated to 900 °C to prevent nozzle clogs. A "pick-up" line placed immediately in front of the nozzle tip introduced an effusive flow of O_2 to be entrained in the expanding jet. A negatively biased hot thoriated iridium filament injected electrons into the expanding jet (at −75 V bias, 10 mA emission current), creating a weakly ionized plasma. A predominantly axial magnetic field was used to confine the plasma and greatly enhanced the anion production. Negative ions were extracted from the ionized jet, accelerated to 500 eV, and transported by a series of ion optics into a Wein velocity filter for mass selection. Although N_2O is typically used to produce monoxide cluster anions, (it produces O^- by dissociative electron attachment more efficiently than does oxygen), during these experiments we used O_2 so that MgO_2^- could also be made abundantly[24] (although the data of MgO_2^- is not reported here). Under these conditions, the ion source produced 20 pA continuous ion current of MgO^- and 5−10 pA MgO_2^-. The mass selected anion beam was focused into a field-free interaction region where it was crossed with an intracavity photon beam of an argon ion laser operated at 488 nm (2.540 eV) at typical circulating powers of 150 W. The distance from the ion source to the ion beam−laser interaction region is ∼2 m. Photoelectrons were collected through a small solid angle defined by the input optics of the hemispherical electron energy analyzer located below the interaction zone. The voltages of the input optics are scanned, and the electron analyzer is operated at a constant pass energy of 5 eV. The electron energy resolution with the hemispherical analyzer is constant. The photoelectron spectra of MgO^- was recorded under a typical resolution of 23 meV (fwhm) and calibrated with the known O^- photoelectron spectrum.[31]

3. Results and Analysis

3.1. MgO^-. The photoelectron spectra of MgO^- taken at PNNL/WSU (532, 355, and 266 nm) and JHU (488 nm) and

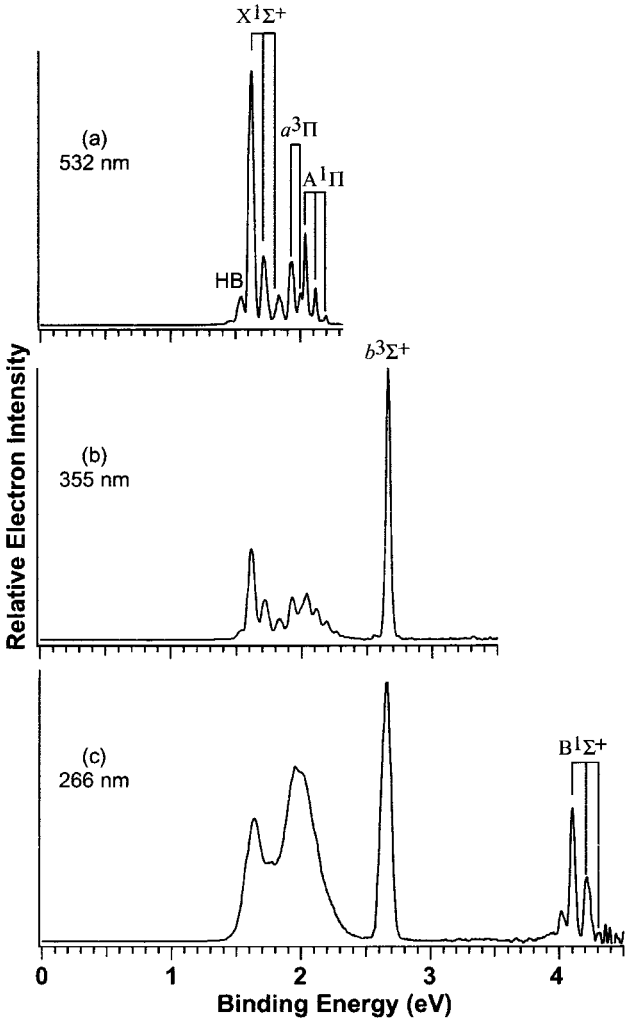

Figure 1. Photoelectron spectra of MgO^- at (a) 532, (b) 355, and (c) 266 nm.

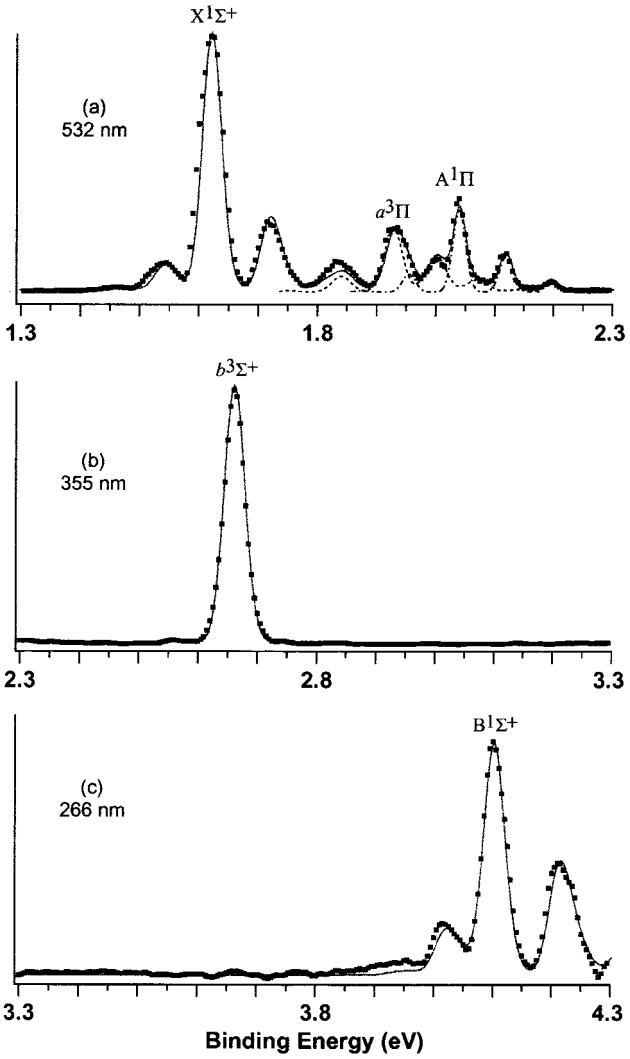

Figure 2. Franck−Condon analysis of the photoelectron spectra of MgO^- obtained at PNNL/WSU. The dots are experimental results, whereas the solid lines represent simulations. Particularly for the 532 nm (a) spectrum, individual fits to excited states are also shown as dotted ($a^3\Pi$) and dot−dashed ($A^1\Pi$) lines, respectively.

the results of Franck−Condon analyses of the data are displayed in Figures 1−4. The detachment energy of the photoelectron peaks corresponding to (0−0) vibrational transitions defines the adiabatic electron affinity for the respective neutral states, within the accuracy of rotational correction. The observed detachment energies and spectroscopic information are summarized in Table 1.

3.1.1. The 532 and 488 nm Spectra, MgO^- ($X^2\Sigma$) → MgO ($X^1\Sigma$, $a^3\Pi$, $A^1\Pi$) + e^-. The 532-nm PNNL/WSU spectrum (Figure 1a) and 488-nm JHU spectrum (Figure 3) are largely consistent, with the notable exception that the spectrum taken at JHU contains an exceptionally high degree of vibrational hot banding. Each spectrum finds photodetachment transitions to the three lowest electronic states of the MgO molecule, the $X^1\Sigma$, $a^3\Pi$, and $A^1\Pi$ states. However, there is a small shift in absolute energies between the two spectra (∼0.020 eV), which is within the experimental uncertainties. The MgO^- ($X^2\Sigma$, $v'' = 0$) → MgO ($X^1\Sigma$, $v' = 0$) "(0−0)" transition in the 532 nm spectrum was measured to be 1.620 (0.025) eV. The detachment energies of the MgO^- ($X^2\Sigma$) → MgO ($a^3\Pi$, $A^1\Pi$) (0−0) transitions are 1.930 and 2.040 eV, respectively, locating these states at T_0 = 2510 and 3390 cm^{-1} above the ground state.

The low intensity MgO^- ($X^2\Sigma$, $v'' = 1$) → MgO ($X^1\Sigma$, $v' = 0$) hot band transition, the (1−0) peak labeled as HB in Figure 1a, falls on the low binding energy side of the intense (0−0) peak. This feature is well resolved in both spectra. Franck−Condon simulation of the well resolved neutral vibrational progression in the X state of the 532-nm spectrum, including the (1−0) hot band transition, gives direct spectroscopic information for the ground state of both MgO and MgO^-. In the Franck−Condon simulation, the equilibrium bond length and anharmonicity constant for the ground-state MgO were taken from ref 8. The fundamental vibrational frequencies of the ground states of MgO and MgO^- were determined to be 780 (40) cm^{-1} and 670 (80) cm^{-1}, respectively. This analysis also provided an r_e value of 1.794 Å for the MgO^- ground state. Accordingly, the information on the anionic ground-state made further Franck−Condon analyses on the observed excited neutral states possible. In Figure 2a, the results of Franck−Condon simulations for the $X^1\Sigma$, $a^3\Pi$, and $A^1\Pi$ states are compared with the experimental data.

3.1.2. The 355 and 266 nm Spectra, MgO^- ($X^2\Sigma^+$) → MgO ($b^3\Sigma^+$, $B^1\Sigma^+$) + e^-. At higher photon energies, photodetachment to two additional MgO excited states, $b^3\Sigma^+$ and $B^1\Sigma^+$, were observed at 2.660 and 4.100 eV, respectively, locating these states at T_0 = 8390 and 20 000 cm^{-1} above the MgO $X^1\Sigma$ ground state. The $b^3\Sigma^+$ feature at 2.660 eV is distinctly different from the others in that it consists only of an intense (0−0) transition with no appreciable neutral vibrational progression,

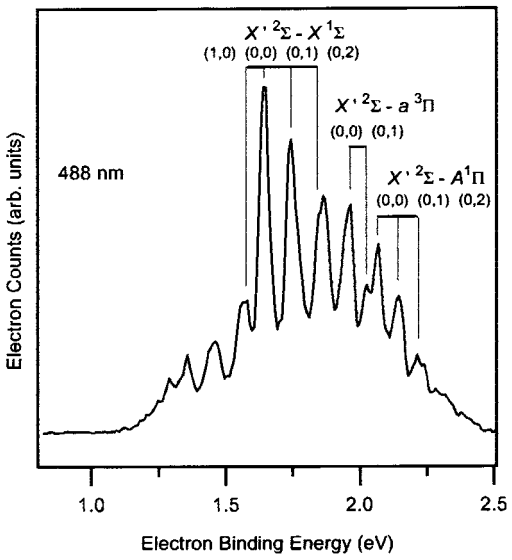

Figure 3. Photoelectron spectra of MgO^- at 488 nm.

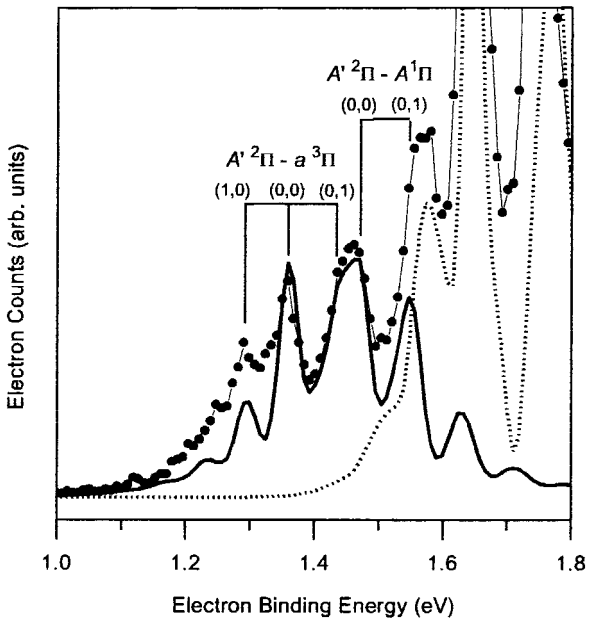

Figure 4. Franck−Condon analysis of the photoelectron spectra of MgO^- obtained at JHU. The solid circles are experimental results, whereas the solid line and dotted line represent simulations.

indicating that there is little change in geometry between this state and the anionic ground state. The r_e value obtained from the Franck−Condon simulation for this state (Figure 2b) is shorter than the anion by only 0.003 Å.

3.1.3. Detachment from a Low-Lying Anion State, MgO^- ($A^2\Pi$) → MgO ($a^3\Pi$, $A^1\Pi$) + e^-. Examination of the low binding energy region of the 488-nm spectrum (Figure 3) finds photodetachment transitions at energies lower than that required to detach an electron from the $X^2\Sigma$ ground-state anion. In fact, these features extend to lower detachment energies than the ground-state anion to ground-state neutral, (1−0), (2−0), ... (ν''-0), hot band transitions, (whose thermally populated higher order intensities drop off exponentially). These are the lowest energy transitions expected for a single anion state. Since the possibility of impurity in the MgO^- beam can be ruled out, the lower binding energy transitions that appear in the spectrum should correspond to detachment from a low-lying electronic state of the anion. A Franck−Condon simulation was performed

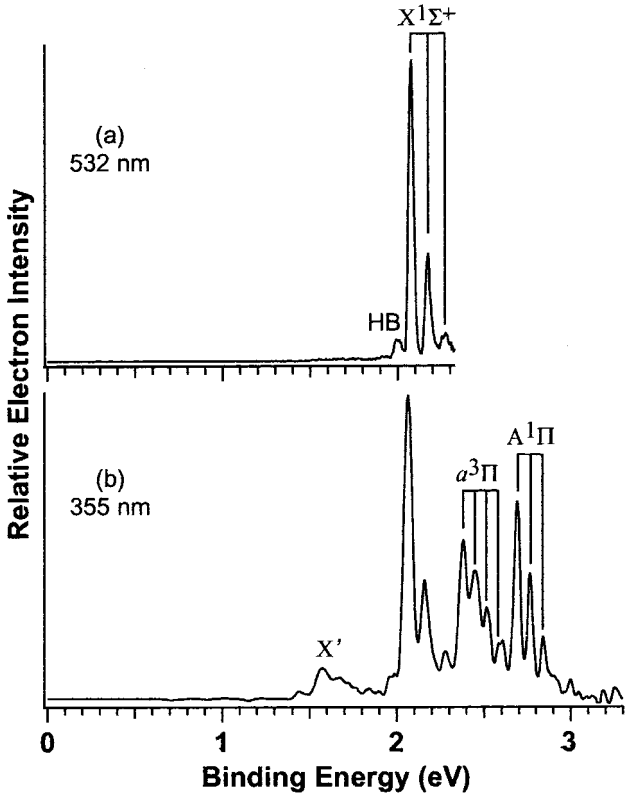

Figure 5. Photoelectron spectra of ZnO^- at 532 and 355 nm.

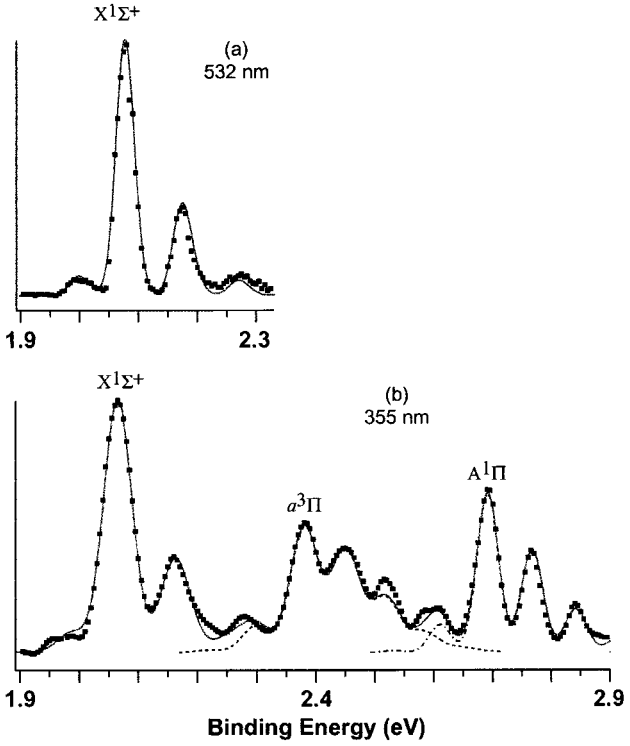

Figure 6. Franck−Condon analysis of the photoelectron spectra of ZnO^- obtained at PNNL/WSU. The dots are experimental results, whereas the solid lines represent simulations. For the 355 nm (b) spectrum, individual fits to excited states are also shown as dotted ($a^3\Pi$) and dot-dashed ($A^1\Pi$) lines, respectively.

for all electronic transitions that appear in the 488-nm spectrum using the neutral state information derived from the above analyses of the colder PNNL/WSU spectra. Franck−Condon analyses of the transitions from the ground-state anion, MgO^-

TABLE 1: Observed Vertical Detachment Energies (VDE) and Spectroscopic Constants of MgO from the Photoelectron Spectra of MgO^-

	VDE (eV)		term value (cm^{-1})[i]				bond length (Å)			vib. freq. (cm^{-1})		
	PNNl	JHU	PNNL	JHU	ref 8[b]	calc.	current	ref 8	calc.	current	ref 8	calc.
MgO^-												
$X^2\Sigma^+$			−13070	−13240		−12561[h]	1.794[e]		1.794[f]	670(80)		897[f]
$(6\sigma^2 2\pi^4 7\sigma^1)$									1.801[h]			739[h]
$A^2\Pi$		0.594(0.023)[g]		−8440		−7711[h]	1.911		1.970[h]	593(80)		512[h]
$(6\sigma^2 2\pi^3 7\sigma^2)$												
MgO												
$X^1\Sigma^+$	1.620[a](0.025)	1.641[a](0.023)	0	0		0		1.749	1.787[d]	780(40)	785	806[d]
$(6\sigma^2 2\pi^4)$									1.771[h]			760[h]
$a^3\Pi$	1.930(0.025)	1.953(0.023)	2510(140)	2520(140)	2623[c]	1929[d]	1.864	1.870	1.908[d]	600(80)	648	615[d]
						1766[h]			1.888[h]			645[h]
$A^1\Pi$	2.040(0.015)	2.062(0.023)	3390(150)	3400(150)	3563	2666[d]	1.854	1.864	1.889[d]	650(80)	664	677[d]
$(6\sigma^2 2\pi^3 7\sigma^1)$						2621[h]			1.884[h]			654[h]
$b^3\Sigma^+$	2.660(0.020)		8390(150)			8414[d]	1.791		1.863[d]	~670		616[d]
$B^1\Sigma^+$	4.100(0.025)		20000(160)		19984	20212[d]	1.730	1.737	1.767[d]	890(80)	824	846[d]
$(6\sigma^1 2\pi^4 7\sigma^1)$												

[a] The measured adiabatic electron affinity of MgO. An average of these two values, EA = 1.630 eV, is within the uncertainty of these measurements (ref 35 gives a theoretical value of 1.639 eV at the CCSD level). [b] Previous experimental values. [c] From ref 1 (experimental). [d] From ref 12, the potential curves calculated using the multireference configuration interaction (MRD CI) method. [e] An optimized value in the Franck−Condon analysis using the bond length of MgO (1.749 Å) given in ref 8. [f] From ref 35 (calculated). [g] MgO^- $A^2\Pi$−MgO $a^3\Pi$ = 1.349 eV and MgO^- $X^2\Sigma$−MgO $a^3\Pi$ = 1.953 eV detachment energies place the $A^2\Pi$ anion 0.594 eV above the $X^2\Sigma^+$ ground state. [h] Calculations from ref 25, the term values have had the "zero" moved from the ground-state anion to the ground-state neutral for comparison purposes. [i] Experimental term values are T_0. Calculated term values are T_e.

TABLE 2: Observed Vertical Detachment Energies (VDE) and Spectroscopic Constants of ZnO from the Photoelectron Spectra of ZnO^-

	VDE (eV)			Term value (cm^{-1})	Bond length (Å)			Vib. freq. (cm^{-1})		
	current	ref 21[b]	ref 22[c]	current	current	ref 21	ref 22	current	ref 21	ref 22
ZnO^-										
$X^2\Sigma^+$				−16750	1.767[d]	1.787	1.764	610	625	664
$(9\sigma^2 4\pi^4 10\sigma^1)$								(80)		
ZnO										
$X^1\Sigma^+$	2.077[a]	2.088	2.03	0			1.719	770	805	727
$(9\sigma^2 4\pi^4)$	(0.020)							(40)		
$a^3\Pi$	2.382	2.338	2.29	2460	1.850		1.857	540		567
	(0.025)			(120)				(80)		
$A^1\Pi$	2.692			4960	1.838		1.848[e]	600		617[e]
$(9\sigma^2 4\pi^3 10\sigma^1)$	(0.015)			(150)				(80)		

[a] The measured adiabatic electron affinity of ZnO. [b] Previous negative ion photoelectron spectroscopy results by Fancher et al. [c] Ab initio calculations at the CCSD(T) level by Bauschlicher and Partridge. [d] An optimized value in the Franck−Condon analysis using the bond length of ZnO (1.719 Å) given in ref 22. [e] A single-reference CI calculation based upon SCF orbitals by Bauschlicher and Langhoff (ref 2).

$(X^2\Sigma) \rightarrow$ MgO ($X^1\Sigma$, $a^3\Pi$, $A^1\Pi$), confirmed that the high-temperature JHU spectrum is consistent with the spectroscopic parameters found from the colder PNNL/WSU 532-nm spectrum. Using the neutral spectroscopic constants obtained from the 532-nm spectrum, a Franck−Condon simulation of the lower binding energy spectral features found that photodetachment of the excited anion electronic state produced a triplet−singlet pair of Π neutral electronic states (Figure 4). The detachment energy of the excited-state anion to the neutral $a^3\Pi$ state was measured to be 1.349 eV. Subtracting this from the MgO^- $X^2\Sigma$−MgO $a^3\Pi$ spacing locates the excited-state anion 0.594 eV above the ground-state anion. With the anion states thus positioned, photodetachment from the excited anion to the $X^1\Sigma^+$ ground-state neutral would appear at 1.047 eV electron binding energy, but was not observed, as is evident in Figure 3. The excited MgO^- anion is expected to have a relatively long lifetime (on the order of 10^{-4} s), because fluorescence lifetimes are inversely proportional to ν^3 and the 0.594 eV radiative transition to the ground-state anion lies in the infrared. Radiative lifetimes and transition moments in neutral MgO have been calculated by Diffenderfer, Yarkony, and Dagdigian.[32] The authors found that the $A^1\Pi - X^1\Sigma^+$ transition (~0.4 eV) has a lifetime of 0.23 ms. Transit time from the ion source to the ion beam−laser interaction region in the JHU photoelectron spectrometer is $\sim 10^{-5}$ s for a 40 amu ion.

3.2. ZnO^-. The 532 and 355 nm photoelectron spectra of ZnO^- taken at PNNL/WSU and the corresponding Franck−Condon analysis results are shown in Figure 5 and Figure 6, respectively. The (0−0) transition to the neutral ground state at 2.077 (0.020) eV is consistent with the adiabatic electron affinity of 2.088 (0.010) eV obtained in the previous 457.9 nm (2.707 eV) photoelectron study at JHU within the experimental uncertainties.[21] The spectroscopic constants obtained from Franck−Condon analyses are also consistent with the prior result and are summarized in Table 2. The greater photon energy range employed in the current study accesses photodetachment transitions to the first two excited states of ZnO. The detachment energies of these two states are found to be 2.382 and 2.692 eV and hence lie at T_0 = 2460 and 4960 cm^{-1} above the ground state, respectively. In addition to the (1−0) hot band transition located at ~2 eV (Figure 5a), spectral features are also observed at lower binding energies (~1.4 eV) in the 355 nm spectrum (labeled X′ in Figure 5b). These features are most likely due to transitions from an excited state of the anion, analogous to that observed in the 488-nm spectrum of MgO^- reported above. It is interesting to note that this feature is not observed in the 532

nm spectrum (Figure 5a), consistent with the assignment to an excited anion, which can be produced only under certain experimental conditions. Due to insufficient resolution and count rates in this region of the 355 nm spectrum, this feature is not subjected to a more detailed analysis.

4. Discussion

4.1. MgO^-/MgO. The $^1\Sigma^+$ states of MgO are not well described by a single configuration. In particular, the $X^1\Sigma^+$ ground state and the $B^1\Sigma^+$ state are composed of varying mixtures of $6\sigma^2 2\pi^4$, $6\sigma^1 2\pi^4 7\sigma^1$, and $6\sigma^1 2\pi^4 3\pi^1$ configurations.[33,34] Peyerminhoff and co-workers find that the $X^1\Sigma^+$ ground state is dominated by the closed-shell $6\sigma^2 2\pi^4$ structure, where 6σ is a bonding orbital derived from Mg 3s and O $2p_z$ atomic orbitals, and 2π has a nonbonding O $2p\pi$ character.[12] Electronic transitions from these occupied orbitals to the 7σ antibonding orbital produces the low lying neutral electronic states, $a^3\Pi$, $A^1\Pi$, $b^3\Sigma$, and $B^1\Sigma$. In the ground-state MgO^- anion, the additional electron occupies the lowest available unoccupied molecular orbital, the 7σ orbital. Electron detachment from the excited state of the MgO^- anion has been found to produce the $a^3\Pi$, $A^1\Pi$ neutral states, but not the $X^1\Sigma^+$ ground state, indicating a predominantly $6\sigma^2 2\pi^3 7\sigma^2$ configuration. All of the detachment channels leading to the states observed in the photoelectron spectra of MgO^- may be described in terms of these configurations as follows:

$$6\sigma^2 2\pi^4 7\sigma^1\ (MgO^-, X^2\Sigma^+) \rightarrow 6\sigma^2 2\pi^4\ (MgO, X^1\Sigma^+) \quad (1)$$

$$\rightarrow 6\sigma^2 2\pi^3 7\sigma^1 (MgO, a^3\Pi, A^1\Pi) \quad (2)$$

$$\rightarrow 6\sigma^1 2\pi^4 7\sigma^1 (MgO, b^3\Sigma^+, B^1\Sigma^+) \quad (3)$$

$$6\sigma^2 2\pi^3 7\sigma^2\ (MgO^-, A^2\Pi) \rightarrow 6\sigma^2 2\pi^3 7\sigma^1 (MgO, a^3\Pi, A^1\Pi) \quad (4)$$

Detachment of an electron from the 7σ orbital of the ground state anion produces the ground state neutral (eq 1). Detachment of the more tightly bound 2π and 6σ electrons produces excited Π (eq 2) and Σ (eq 3) states, respectively, each with a triplet−singlet splitting due to detachment of either an α or β electron. Detachment of an electron from the 7σ orbital of the excited-state anion produces the Π states with a triplet−singlet splitting due to detachment of either an α or β electron (eq 4). Electronic configurations, detachment energies and spectroscopic constants are collected in Table 1 and compared with literature values where available. The 1.630 eV adiabatic electron affinity we report is in good agreement with the calculation of Gutsev et al. (1.639 eV) at the CCSD level of theory.[35] The vibrational frequency for the MgO $X^1\Sigma^+$ ground-state found by these investigators ($\omega_e = 818$ cm^{-1}) compares reasonably well to that obtained here, $\omega_e = 780$ cm^{-1}. IR spectra measured from matrix reactions of magnesium with various oxidants (O_2, O_3, and N_2O) in solid argon and solid nitrogen by Andrews et al.[36,37] found similar results, with values ranging from 787 to 825 cm^{-1}. Relative dissociation energies may be derived from the vertical detachment energies of the corresponding (0−0) peaks in the photoelectron spectra by a thermochemical cycle, $\Delta T_0 + \Delta D_0 = \Delta E$ (dissociation asymptotes), and are discussed in the sections that follow.

4.1.1. The $X^1\Sigma^+$ Ground State. For predominantly ionic molecules such as MgO, strongly bound ionic potential curves, whose dissociation asymptotes lie above the neutral separated atoms, cross mostly repulsive covalent curves, producing avoided crossings at some intermediate distance for curves of the same symmetry. Ionic and covalent diabats and the resultant potential curves for the low-lying states of MgO have been calculated using a multireference configuration interaction (MRD-CI) method in an extensive study of the electronic structure of the MgO molecule by Thümmel, Klotz, and Peyerminhoff.[12] This work included a thorough investigation of the covalent−ionic interactions at long internuclear distances where the avoided crossings occur. The bonding in ground-state MgO, a state with $^1\Sigma$ symmetry and noted for its multiconfigurational nature, thus arises predominantly from an avoided crossing of the ionic curve dissociating to Mg^+ (^{2}S) + O^- (^{2}P) and the covalent curve associated with the singlet atomic oxygen limit, Mg (^{1}S) + O (^{1}D). The bonding in the first excited molecular state, the $a^3\Pi$ state, arises from an avoided crossing between curves derived from the ionic Mg^+ (^{2}S) + O^- (^{2}P) asymptote and the covalent potential associated with triplet oxygen, the ground state separated atoms Mg (^{1}S) + O (^{3}P). To derive a thermochemical value of the dissociation energy of MgO, the energy spacing between the ground state and the first excited state, measured from the photoelectron spectra, $T_0(a^3\Pi) = 0.310$ eV, was added to the $D_e(a^3\Pi) = 1.82$ eV calculated by Thümmel et al. (neglecting zero point energy, which is on the order of a few meV). From this estimation we obtain a thermochemical dissociation energy of 2.13 eV, for dissociation to ground-state atoms. This is consistent with, though somewhat lower than, recent experimental[15] and theoretical[14] results, 2.56 and 2.71 eV, respectively. As in prior experimental and theoretical work, these determinations of the dissociation energy neglect the triplet-to-singlet atomic oxygen promotion energy needed to reach the asymptote to which the $X^1\Sigma^+$ state dissociates. Including the 1.97 eV atomic oxygen $O(^3P)-O(^1D)$ transition energy, we find that D_0 ($X^1\Sigma^+$) = 4.10 eV, dissociating to its natural dissociation products, Mg (^{1}S) + O (^{1}D). Experimental dissociation energy values from flame photometry assuming a $X^1\Sigma^+$ ground state[8,13] find $D_0 = 4.34$ and 4.14 eV, in good agreement with our result.

4.1.2. The $a^3\Pi$ and $A^1\Pi$ States. Bonding in the triplet and singlet Π states arises from avoided crossings between the ionic Mg^+ (^{2}S) + O^- (^{2}P) potential, and covalent curves dissociating to ground-state triplet and singlet atomic oxygen, Mg (^{1}S) + O (^{3}P), and Mg (^{1}S) + O (^{1}D). With the Π molecular states measured to be only 0.110 eV apart and with separated atom limits 1.97 eV apart, we find that the dissociation energy of the $A^1\Pi$ state is 1.86 eV larger than that of the $a^3\Pi$ state. Referenced to $D_e(a^3\Pi) = 1.82$ eV[12] (again, neglecting zero point energy) we find $D_0(A^1\Pi) = 3.68$ eV. The Π state vibrational frequencies are significantly lower and equilibrium bond lengths longer than that of the $^1\Sigma$ ground state; $\omega_e(a^3\Pi) = 600$ cm^{-1}, $\omega_e(A^1\Pi) = 650$ cm^{-1} vs $\omega_e(X^1\Sigma^+) = 780$ cm^{-1}, and $r_e(a^3\Pi) = 1.864$ Å, $r_e(A^1\Pi) = 1.854$ Å referenced to $r_e(X^1\Sigma^+) = 1.749$ Å.[8] The relative vibrational frequencies, equilibrium bond lengths, and well depths are consistent with promotion of an electron from the bonding 2π orbital to the antibonding 7σ orbital.

4.1.3. The $b^3\Sigma^+$ and $B^1\Sigma^+$ States. The Σ pair of excited molecular states, $b^3\Sigma^+$ and $B^1\Sigma^+$, observed in the 355 and 266 nm photoelectron spectra, show an unusual behavior in that their triplet−singlet splitting is considerable (1.440 eV) and the spectral envelope of each state does not exhibit any similarity. Indeed, there has been no experimental observation of the $b^3\Sigma^+$ state prior to this study, which appears as a sharp (0−0) peak at 2.66 eV in our photoelectron spectra with no appreciable vibrational progression, (note the very low intensity feature indicative of the (0−1) transition at ~2.75 eV in Figure 2b).

Because photodetachment is a vertical process that accesses the neutral at the geometry of the anion, the lack of a vibrational progression for the $b^3\Sigma^+$ neutral state indicates that this neutral state has a geometry (bond length and well shape) similar to that of the ground-state anion. The equilibrium bond length found from the Franck−Condon simulation, $r_e(MgO, b^3\Sigma^+) = 1.791$ Å vs $r_e(MgO^-, X^2\Sigma^+) = 1.794$ Å, is consistent with this expectation. With only a trace intensity for the (0−1) peak, we are not able to confidently report a vibrational frequency for the $b^3\Sigma^+$ state but expect it to be similar to that of the ground-state anion (670 cm^{-1}).

Unlike the $b^3\Sigma^+$ state, the spectral profiles of the $B^1\Sigma^+$ singlet state detachment transitions show a vibrational progression with a relatively intense (0−1) peak, indicating that the geometry of the $B^1\Sigma^+$state is significantly different from that of the ground-state anion. The shorter bond length and higher vibrational frequency found from the Franck−Condon simulation is consistent with this expectation, $r_e(B^1\Sigma^+) = 1.730$ Å, $\omega_e(B^1\Sigma^+) = 890$ cm^{-1} vs $r_e(MgO^-, X^2\Sigma^+) = 1.794$ Å, $\omega_e(MgO^- X^2\Sigma^+) = 670$ cm^{-1}. Thus, the photoelectron spectra find that the potential curves for these two excited Σ states have significantly different spectroscopic characteristics and energetics. In contrast, the Π triplet−singlet pair, discussed previously, lie close in energy (0.110 eV) and have similar vibrational frequencies and equilibrium bond lengths. A viable explanation for the behavior of the Σ states can be given based upon the set of potential energy curves and transformed diabats calculated for MgO in ref 12. The avoided crossing, involved in the potential curve for the $b^3\Sigma^+$ state, was analyzed from an ionic diabat and a covalent counterpart whose electronic configurations and dissociation limits are as follows:

$$MgO\ (6\sigma^1 2\pi^4 7\sigma^1) \rightarrow Mg^+\ (3s^1, {}^2S) + O^-\ (2p,^5\ {}^2P)\ \text{(ionic)}$$

$$MgO\ (6\sigma^1 2\pi^3 7\sigma^1 3p\pi^1) \rightarrow Mg\ (3s^1 3p^1, {}^3P) + O\ (2p,^4\ {}^3P)\ \text{(covalent)}$$

As is typical in avoided crossings of ionic molecules, the ionic curve will provide the major contribution at short internuclear separations, whereas the repulsive covalent diabat plays an important role at longer internuclear distances. The CI expansion results in ref 12 also indicate that this $6\sigma^1 2\pi^4 7\sigma^1$ configuration is the dominant component (about 90%) at the equilibrium distance in a proper CI description of the $b^3\Sigma^+$ state. Hence it is reasonable to approximate the equilibrium configuration of MgO in the $b^3\Sigma^+$ state to be the $6\sigma^1 2\pi^4 7\sigma^1$ ionic configuration. In contrast, the $B^1\Sigma^+$ state at the equilibrium distance has appreciable contribution from ionic potentials of configuration $6\sigma^2 2\pi^3 3p\pi^1$ [Mg^+ (^2P) + O^- (^2P)] and $6\sigma^2 2\pi^4$ [Mg^{2+} (^1S) + O^{2-} (^1S)], in addition to the $6\sigma^1 2\pi^4 7\sigma^1$ configuration. As expected for an ionic molecule, the character of the orbitals involved in these configurations changes with internuclear distance. These have been examined by Peyerimhoff and co-workers,[12] who find that the 6σ orbital has a $2p_z$(O) character at short distance and a bonding 2pσ(O) + 3s(Mg) character at intermediate distance. The 7σ orbital was found to have a semidiffuse 3s(Mg) slightly antibonding character, which evolves to the antibonding 2pσ(O)−3s(Mg) linear combination at intermediate distance. The singlet $B^1\Sigma^+$ state, with less contribution from the 7σ orbital, may be expected to have increased bonding character relative to the triplet $b^3\Sigma^+$ state. Thus, the longer equilibrium distance for the triplet state (1.791 Å vs 1.730 Å) can be understood through comparison with the singlet as discussed above.

4.1.4. The Ground State of MgO^-, $X^2\Sigma^+$. As discussed earlier, neutral MgO has molecular orbitals ordered 6σ, 2π, 7σ, where the 2π molecular orbital has mainly O 2pπ character and the 6σ and 7σ orbitals are the bonding and antibonding σ molecular orbitals derived from the Mg 3s and O $2p_z$ atomic orbitals. The ground-state anion is formed by electron addition to the lowest unoccupied molecular orbital and thus has a $6\sigma^2 2\pi^4 7\sigma^1$ configuration. With three σ electrons, this configuration corresponds to the Mg(^1S) + O^-(^2P) ion−neutral dissociation limit with the "hole" in the O^- $2p^5$ subshell located along the internuclear axis, a $^2\Sigma^+$ molecular anion state. Here the 6σ and 7σ molecular orbitals are expected to have mainly O $2p_z^1$ + Mg $3s^2$ character. Through a thermochemical cycle, as described earlier, the anion dissociation energy is found to be $D_0(MgO^-, X^2\Sigma) = 2.289$ eV, significantly lower than that of the ground-state neutral. Franck−Condon simulation of the 532 nm MgO^- spectrum finds a longer anion bond length, and lower anion vibrational frequency. These results are consistent with electron addition to an antibonding orbital. The bonding in neutral MgO is due to the interaction of ionic $Mg^+ + O^-$ potentials and repulsive covalent Mg + O potentials. For the molecular anion, the "covalent" curve is the ion−neutral interaction which will also be mostly repulsive with a shallow well at long bond length. For example $D_0(O^-Ar, X^2\Sigma) = 0.097$ eV.[24] Thus in MgO^-, additional anion stabilization is expected from avoided crossings with $Mg^+ + O^{2-}$ charge-transfer potentials of $^2\Sigma^+$ symmetry, analogous to the role played by the ionic curves in neutral MgO. The lowest energy charge-transfer asymptote for the molecular anion is Mg^+ ($3s^1$, ^2S) + O^{2-} ($2p_z^2 p_{x,y}^4$, ^1S), which produces a $^2\Sigma$ molecular state. Like the ion−neutral Mg + O^- limit, this charge-transfer limit corresponds to a $6\sigma^2 2\pi^4 7\sigma^1$ configuration, though here the 6σ and 7σ molecular orbitals are expected to have mainly O^{2-} $2p_z^2$ + Mg^+ $3s^1$ character. With similar molecular orbital occupancies, the ion−molecule and charge-transfer configurations are expected to have the same qualitative photodetachment behavior. Thus the stabilizing influence of the charge-transfer limit in the bonding of the ground-state anion is evident in our photoelectron spectrum from the measured detachment energies (from which we derive relative dissociation energies).

Further light may be shed upon the bonding in the ground-state MgO^- anion by reference to the CCSD(T) calculation of the similar ZnO and ZnO^- system.[22] The analogous valence molecular orbitals in ZnO are 9σ, 4π, 10σ. As in MgO the 4π orbital was found to be mainly O 2pπ, with some donation to Zn. In molecular states with 3 σ electrons, for example ZnO $a^3\Pi$ ($9\sigma^2 4\pi^3 10\sigma^1$) and ZnO^- $^2\Sigma$ ($9\sigma^2 4\pi^4 10\sigma^1$), the Zn atom was found to undergo 4s4p hybridization to form σ and σ* orbitals with O $2p_z$. This σ bonding was found to be enhanced by 2pπ donation. Consequently, the ZnO^- anion, with an additional 2pπ electron, was found to be more strongly bound, with a more covalent and less ionic σ character, than the ZnO $a^3\Pi$ neutral. Because the ZnO $X^1\Sigma$ ($9\sigma^2 4\pi^4$) state has only two σ electrons, no promotion energy is required for Zn hybridization and the ZnO $X^1\Sigma$ ground state was found to be stronger than either ZnO $a^3\Pi$ neutral or ZnO^- $X^2\Sigma$ anion. Interestingly, the relative dissociation energies found from the photodetachment of the analogous MgO and MgO^- states in this work follow the same trend, $D_0(MgO, X^1\Sigma) = 4.10$ eV > $D_0(MgO^-, X^2\Sigma) = 2.29$ eV > $D_0(MgO, a^3\Pi) = 1.82$ eV, and indicate that a similar bonding interaction is occurring in MgO and MgO^-.

4.1.5. The Excited State of MgO^-, $A^2\Pi$. When the singly occupied O^- 2p orbital is oriented perpendicular to the internuclear axis, the Mg ($3s^2$, ^1S) + O^- ($2p_z^2$ $p_{x,y}^3$, ^2P) ion−neutral

limit gives rise to a $^2\Pi$ state. With four σ and three $2p\pi$ electrons, this limit corresponds to a MgO^- $6\sigma^2 2\pi^3 7\sigma^2$ configuration. Photodetachment of a 7σ electron produces the $6\sigma^2 2\pi^3 7\sigma^1$ ($a^3\Pi$, $A^1\Pi$) neutral states as the lowest detachment energy electronic transitions. Notice that single electron detachment does not produce the neutral $6\sigma^2 2\pi^4$ ground state configuration. Consequently, we assign the excited-state anion observed in the 488 nm MgO^- photoelectron spectrum to an $A^2\Pi$ state. Because both the $X^2\Sigma$ and $A^2\Pi$ MgO^- states dissociate to the Mg (^1S) + O^- (^2P) limit (neglecting spin−orbit splitting), the difference in their transition energies, 0.594 eV, is also the difference in their dissociation energies. Thus, $D_0(MgO^-, A^2\Pi) = 1.70$ eV. Although this dissociation energy is weaker still than the ground state anion, the interaction is still significantly stronger than an unalloyed ion-induced dipole interaction, where, for example, D_0 (O^-Ar $^2\Pi$) = 0.064 eV.[24] Thus, additional anion stabilization is expected from avoided crossings with charge-transfer potentials of $^2\Pi$ symmetry. The lowest energy charge-transfer limit with $^2\Pi$ symmetry is Mg^+ ($3p^1$, ^2P) + O^{2-} ($2p,^6$ ^1S), corresponding to a $6\sigma^2 2\pi^4 7\sigma^0 3\pi^1$ configuration, where the 3π orbital has mainly Mg 3p character. This configuration photodetaches to the $6\sigma^2 2\pi^4$ MgO $X^1\Sigma$ ground-state neutral, which is not observed in our photoelectron spectrum. This would appear to indicate that the bonding region of MgO^- is primarily described by the Mg + O^- ion−neutral limit with significant, if not predominant, contribution from the charge transfer limit. There are no analogous experimental investigations for the excited anion state with which to compare these results. However, the neutral alkaline earth halides and hydroxides have been investigated both experimentally and theoretically and are isoelectronic with MgO^-. The bonding in MX (M = alkaline earth metal, X = halogen or hydroxide radical) is highly ionic and is generally envisioned as M^{2+} + X^- + e^-, with the electron localized mainly in an $n\sigma^1$ nonbonding (M s^1) orbital in the MX (X $^2\Sigma$) ground state. Low lying electronic states are formed by promotion of the $n\sigma$ metal electron to the M $np\pi$ orbital to produce the $A^2\Pi$ state or to the M $np\sigma$ orbital to produce the $B^2\Sigma$ state. In the $^2\Sigma$ ground state, it has been found that the covalent character of the bond increases with diminishing size of the alkaline earth atom (as the IP of the metal increases) with the transition from predominantly ionic to covalent occurring at Mg.[38−40] Comparing hyperfine constants for MgF to fluorides of heavier alkaline earth metals, the unpaired electron in MgF was found to have slightly more density on the fluorine atom than the metal atom, indicating a greater degree of covalent character for diatomic MgF.[38] Bauschlicher and coworkers calculated the structure and energetics of ground-state alkaline earth monohydroxides[39] and the dipole moments of the alkaline earth fluorides and chlorides.[40] Ca, Sr, and Ba hydroxides were found to be linear, as expected for an electrostatic interaction. MgOH was found to be linear with a flat bending potential, and BeOH was found to be bent, θ = 147°, as expected for a covalent interaction. In the dipole moment study, the calcium monhalides were found to be predominantly ionic, whereas BeF and BeCl were found to show signs of covalent character. For MgO^-, the degree of "covalent" character (in the anion case, ion-induced dipole character) is expected to be greater than in neutral MgX, where the high electron affinity of the halogen favors ionic bonding. The question is, to what extent is an electron transferred to the oxygen anion from neutral magnesium, since, unlike the halogen anions, O^{2-} is not a stable gas phase species. Clearly, O^- anion is not as willing to accept electron density as a fluorine atom. Consequently, we expect the charge-transfer contribution to the configuration of the MgO^- anion states to be significant but under 50%. A predominantly Mg + O^-, $6\sigma^2 2\pi^3 7\sigma^2$, configuration for the MgO^- $A^2\Pi$ state is consistent with the detachment observed in the 488 nm photoelectron spectrum. The experimental observations and conclusions drawn from them are consistent with the results of Bauschlicher and Partridge[25] who calculated spectroscopic constants for the MgO^- $A^2\Pi$ excited anion (in addition to the $X^2\Sigma$ ground state as discussed previously). These are summarized in Table 1. The agreement between the term energies is particularly good, with $T_0(MgO^-$ $A^2\Pi$, exp.) and $T_e(MgO^-$ $A^2\Pi$, calc.) found to lie 4800 and 4850 cm^{-1} above the T_0 and T_e of the ground-state anion, respectively. In addition, Bauschlicher and Partridge have calculated electron detachment overlaps between the two anion states and neutral MgO states. They find that there is essentially zero overlap between the MgO^- $A^2\Pi$ anion and the $X^1\Sigma^+$ neutral state, as found experimentally.

4.2. ZnO. In earlier theoretical work by Bauschlicher and Partridge,[2] the ground state of ZnO molecule was assigned as a $^1\Sigma^+$ state with a closed-shell electronic structure. They also calculated the spectroscopic properties and dipole moments of three lowest excited states ($a^3\Pi$, $A^1\Pi$, and $b^3\Sigma^+$) of the ZnO molecule, using CI and CPF methods. However, the accuracy of their result was limited by insufficient consideration of electronic correlations. Boldyrev and Simons performed an extensive ab initio study of the bonding of between Zn and all first and second row elements. These calculations confirmed the $X^1\Sigma^+$ ground state for ZnO and provided spectroscopic constants for this and the first three excited triplet states of ZnO neutral.[41] Recent papers on the photoelectron spectroscopic study of ZnO^- [21] and the accompanying theoretical investigation refined at the CCSD(T) level for ZnO and ZnO^- by Bauschlicher and Partridge[22] confirmed the $X^1\Sigma^+$ ground state for ZnO. In addition, very recently the electronic structure of 3d metal monoxide anions were calculated using density functional theory by Gutsev, Rao, and Jena.[42] Their spectroscopic constants for the ground-state ZnO^- anion are consistent with the past photoelectron and CCSD(T) results. Accordingly, the detachment channels for the three transitions observed in our photoelectron spectra (Figure 5) are given as follows:

$$9\sigma^2 4\pi^4 10\sigma^1 (ZnO^-, X^2\Sigma^+) \rightarrow 9\sigma^2 4\pi^4 (ZnO, X^1\Sigma^+) \quad (5)$$

$$\rightarrow 9\sigma^2 4\pi^3 10\sigma^1 (ZnO, a^3\Pi, A^1\Pi) \quad (6)$$

In addition, the weak signals attributed to an excited ZnO^- state are expected to be due to the following detachment transition:

$$9\sigma^2 4\pi^3 10\sigma^2 (ZnO^-, A^2\Pi) \rightarrow 9\sigma^2 4\pi^3 10\sigma^1 (ZnO, a^3\Pi, A^1\Pi) \quad (7)$$

In the 355-nm spectrum (Figure 5b), the term values for the two Π states are measured to be 2460 and 4960 cm^{-1}, respectively. The term value for $a^3\Pi$ reported here is greater than the 0.25 eV (2020 cm^{-1}) value tentatively assigned in the earlier ZnO^- study by Fancher et al., which was inferred indirectly from the deviation of the simulated Franck−Condon factors at high binding energy. Current Franck−Condon analysis for the 355-nm spectrum (Figure 6) shows that there is significant contribution from hot band transitions close to the previously reported (0-0) transition energy of the first excited state, which may have been responsible for the prior Franck−Condon fit deviations in that region. Hence, both of the Π excited states have not been observed experimentally prior to the present result. It seems that the theoretical prediction by Baschlicher et al.[22] also somewhat underestimated the term value of the $a^3\Pi$ state. However, r_e and ω_e values are in good

agreement with those obtained from the Franck−Condon analyses of the current ZnO^- photoelectron spectra as can be seen in Table 2.

Note that a considerable broadening in the 355 nm photoelectron spectrum exists in the $a^3\Pi$ state compared with the two singlet states. This kind of broadening effect is often observed in nonsinglet states and can be rationalized by means of ordinary multiplet structures from spin−orbit interaction in diatomic molecules. That is, if the splitting between multiplets is smaller than our experimental resolution, it would not be possible to discriminate the triplet structures in the photoelectron spectra. Looking back upon the $a^3\Pi$ state for MgO in the 532-nm photoelectron spectrum, we find less noticeable broadening due not only to the lighter constituent metal atom, but also to the smaller triplet−singlet splitting between the two Π states of MgO, which made it difficult to appreciate the broadening. Though there is not any measured or calculated value for the spin−orbit coupling constant of the $a^3\Pi$ state of ZnO, we can set a lower and upper limit by taking both the coupling constant of MgO and our typical experimental resolution in the corresponding electron kinetic energy range into account. Most experimental coupling constants of MgO range within 60−70 cm^{-1}.[1,10,11] For photoelectrons of about 1 eV kinetic energy, the resolution is measured to be around 240 cm^{-1} (~30 meV, fwhm). Therefore, we can suggest that the coupling constant of the $a^3\Pi$ state ZnO lies between 60 and 120 cm^{-1}.

5. Conclusions

The vibrationally resolved photoelectron spectra of MgO^- and ZnO^- are presented. Electron affinities, low-lying electronic states for both the anions and neutral, and related spectroscopic constants are reported. Four low-lying excited states are observed for MgO, whereas two are observed for ZnO. An excited anionic state is also observed and analyzed for MgO^-. The well-resolved photoelectron data reported here provide new spectroscopic information for the two seemingly simple diatomic molecules and allows their electronic structure to be well characterized.

Acknowledgment. The authors thank C. W. Bauschlicher and H. Partridge for pursuing calculations of MgO/MgO^- and generously sharing the results prior to publication. The authors are also grateful to C. W. Bauschlicher, R. W. Field, D. R. Yarkony, G. L. Gutsev, and A. I. Boldyrev for helpful discussions. J.H.K. acknowledges a grant from the U.S. Study Visit Program for Graduate Students by the Ministry of Science and Technology of Korea. L.S.W. acknowledges support for this work by The U.S. Department of Energy, Office of Basic Energy Sciences, Chemical Science Division. Part of this work was performed at the W. R. Wiley Environmental Molecular Sciences Laboratory, a national scientific user facility sponsored by the DOE's Office of Biological and Environmental Research and located at Pacific Northwest National Laboratory, operated for DOE by Battelle. L.S.W. is an Alfred P. Sloan Foundation Research Fellow. K.H.B. acknowledges support for this work by the Department of Energy, Division of Materials Science, Office of Basic Energy Sciences under grant number DE-FG02-95ER45538. Acknowledgment is also made to The donors of the Petroleum Research Fund, administered by The American Chemical Society, for partial support of this research under grant number 28452-AC6.

References and Notes

(1) Ikeda, T.; Wong, N. B.; Harris, D. O.; Field, R. W. *J. Mol. Spectrosc.* **1977**, *68*, 452.
(2) Bauschlicher, C. W.; Langhoff, S. R. *Chem. Phys. Lett.* **1986**, *126*, 163.
(3) Schamps, J.; Lefebvre-Brion, H. *J. Chem. Phys.* **1972**, *56*, 573.
(4) Field, R. W. *J. Chem. Phys.* **1974**, *60*, 2400.
(5) Bauschlicher, C. W.; Silver, D. M., Yarkony, D. R. *J. Chem. Phys.* **1980**, *73*, 2867.
(6) Bauschlicher, C. W.; Lengsfield, B. H.; Silver, D. M.; Yarkony, D. R. *J. Chem. Phys.* **1981**, *74*, 2379.
(7) Pearson, P. K.; O'Neil, S. V.; Schaefer, H. F., III *J. Chem. Phys.* **1972**, *56*, 3938.
(8) Huber, K. P.; Herzberg, G. *Molecular Spectra and Molecular Structure IV: Constants of Diatomic Molecules*; Van Nostrand Reinhold: New York, 1979.
(9) Mürtz, P.; Richter, S.; Pfelzer, C.; Thümmel, H.; Urban, W. *Mol. Phys.* **1994**, *82*, 989.
(10) Mürtz, P.; Thümmel, H.; Pfelzer, C.; Urban, W. *Mol. Phys.* **1995**, *86*, 513.
(11) Ip, P. C. F.; Cross, K. J.; Field R. W.; Rostas, J.; Bourguignon, B.; McCombie, J. *J. Mol. Spectrosc.* **1991**, *146*, 409.
(12) Thümmel, H.; Klotz, R.; Peyerimhoff, S. D. *Chem. Phys.* **1989**, *129*, 417.
(13) Pedley, J. B.; Marshall, E. M. *J. Phys. Chem. Ref. Data* **1983**, *12*, 967.
(14) Langhoff, S. R.; Bauschlicher, C. W.; Partridge, H. *J. Chem. Phys.* **1986**, *84*, 4474.
(15) Operti, L.; Tews, E. C.; MacMahon, T. J.; Freiser, B. S. *J. Am. Chem. Soc.* **1989**, *111*, 9152.
(16) Brewer, L.; Mastick, D. F. *J. Chem. Phys.* **1951**, *19*, 834.
(17) Wicke, B. G. *J. Chem. Phys.* **1983**, *78*, 6036.
(18) Clemmer, D. E.; Dalleska, N. F.; Armentrout, P. B. *J. Chem. Phys.* **1991**, *95*, 7263.
(19) Prochaska, E. S.; Andrews, L. *J. Chem. Phys.* **1980**, *72*, 6782.
(20) Chertihin, G. V.; Andrews, L. *J. Chem. Phys.* **1997**, *106*, 3457.
(21) Fancher, C. A.; de Clercq, H. L.; Thomas, O. C.; Robinson, D. W.; Bowen, K. H. *J. Chem. Phys.* **1998**, *109*, 8426.
(22) Bauschlicher, C. W.; Partridge, H. *J. Chem. Phys.* **1998**, *109*, 8430.
(23) Gutowski, M.; Skurski, P.; Li, X.; Wang, L. S. *Phys. Rev. Lett.* **2000**, *85*, 3145.
(24) de Clercq, H. L. Ph.D. thesis, The Johns Hopkins University, 1997. Fancher, C. A. Ph.D. thesis, The Johns Hopkins University, 1997.
(25) Bauschlicher, C. W.; Partridge, H. *Chem. Phys. Lett.*, in press.
(26) Wang, L. S.; Cheng, H. S.; Fan, J. *J. Chem. Phys.* **1995**, *102*, 9480.
(27) Wang, L. S.; Wu, H. In *Advances in Metal and Semiconductor Clusters*; Duncan, M. A., Ed.; JAI Press: Greenwich, 1998; vol. 4, pp 299−343.
(28) Coe, J. V.; Snodgrass, J. T.; Freidhoff, C. B.; McHugh, K. M.; Bowen, K. H. *J. Chem. Phys.* **1986**, *84*, 618.
(29) Feigerle, C. S.; Corderman, R. R.; Bobashev, S. V.; Lineberger, W. C. *J. Chem. Phys.* **1981**, *74*, 1580.
(30) Moore, C. E. *Atomic Energy Levels*; Vol. I−III, National Bureau of Standards Circulation, U.S. GPO: Washington, DC, 1971.
(31) Neumark, D. M.; Lykke, K. R.; Andersen, T.; Lineberger, W. C. *Phys. Rev. A* **1985**, *32*, 1890.
(32) Diffenderfer, R. N.; Yarkony, D. R.; Dagdigian, P. J. *J. Quant. Spectrosc. Radiat. Transfer* **1983**, *29*, 329.
(33) Diffenderfer, R. N.; Yarkony, D. R. *J. Phys. Chem.* **1982**, *86*, 5098.
(34) Yarkony, D. R. *J. Chem. Phys.* **1988**, *89*, 7324.
(35) Gutsev, G. L.; Nooijen, M.; Bartlett, R. J. *Chem. Phys. Lett.* **1997**, *276*, 13.
(36) Andrews, L.; Prochaska, E. S.; Ault, B. S. *J. Chem. Phys.* **1978**, *69*, 556.
(37) Andrews L.; Yustein, J. T. *J. Phys. Chem.* **1993**, *97*, 12700.
(38) Anderson, M. A.; Allen, M. D.; Ziurys, L. M. *J. Chem. Phys.* **1994**, *100*, 824.
(39) Bauschlicher, C. W.; Langhoff, S. R.; Partridge, H. *J. Chem. Phys.* **1986**, *84*, 901.
(40) Langhoff, S. R.; Bauschlicher, C. W.; Partridge, H.; Ahlrichs, R. *J. Chem. Phys.* **1986**, *84*, 5025.
(41) Boldyrev, A. I.; Simons, J. *Mol. Phys.* **1997**, *92*, 365.
(42) Gutsev, G. L.; Rao, B. K.; Jena, P. *J. Phys. Chem.* **2000**, *97*, 5374.